

## CHARACTERISATION OF OXIDES BY ADVANCED TECHNIQUES

Jan Duchoň<sup>1)\*</sup>, Patricie Halodová<sup>1)</sup>, Jan Lorinčínek<sup>1)</sup>, Fosca Di Gabriele<sup>1)</sup>, Anna Hojná<sup>1)</sup>

<sup>1)</sup>Centrum Výzkumu Řež, Husinec-Řež, Czech Republic, EU

Received: 06.11.2017

Accepted: 27.11.2017

\*Corresponding author: e-mail: jan.duchon@cvrez.cz, Tel.: +420 266 173 487, Centrum Výzkumu Řež, Hlavní 130, 250 68 Husinec-Řež, Czech Republic, EU

### Abstract

For the safe development of GenIV nuclear reactors, it is necessary to study the compatibility of structural materials with new coolants. Current work describes the behavior of ferritic-martensitic steel T91 in a Heavy Liquid Metal environment. Specimens were pre-stressed up to yield strength and subsequently exposed to the lead-bismuth eutectic (LBE) under static conditions for 2000 hours. The goal was to identify the susceptibility to crack initiation under selected experimental conditions. The examination of metal-LBE interface was done in a reference position of the sample using the SEM equipped with EDX. Formation of oxide scales observed on the interface had no signs of crack initiation. The oxide was characterized by a two-layer structure. A TEM lamella was created from the sample by a FIB in-situ lift-out technique and it was subsequently analyzed in HRTEM. Individual oxide layers were identified and characterized by SAED, EELS and EDS techniques. Finally, STEM-HAADF and EFTEM techniques were used to visualize the matrix-oxide interface.

**Keywords:** FIB lamella, STEM-EELS, oxidation, ferritic-martensitic steel

### 1 Introduction

Heavy liquid metals are considered as potential coolants in fast reactor designs and have potentially advantageous physical and thermal-hydraulic properties [1-4]. The primary factor limiting the technological viability of the Pb and Pb-Bi eutectic is their corrosive nature towards structural steels. Such coolant has tendency to corrode/dissolute alloying elements from the fuel cladding and structural materials [1, 5-9] within the reactor and causes liquid metal embrittlement (LME) [1, 10-14].

Oxide scales are known to be able to protect the structural alloys against the liquid metal corrosion [1, 7]. The stability of this surface barrier and its long-term protective properties depend on the oxygen content in the environment (coolant) and mainly on the composition and microstructure of the exposed steel [15-18].

This work focuses on the evaluation of oxides developed on the steel T91 exposed to LBE. The oxide layer was characterized in detail by means of TEM, using a lamella prepared by the FIB in-situ lift-out technique.

### 2 Experimental and methods

The ferritic-martensitic steel T91, (Grade 91 Class 2/S50460) of nominal composition (wt. %) Fe-8.9Cr-0.9Mo-0.4Mn-0.2Si-0.2V produced by Industeel, Arcelor Mittal group [19], was used for this experiment.

Specimens from the T91 steel were fabricated by electrical discharge machining (EDM). The surface was ground to 600 grit finish. Specimens with dimensions of 14.9x3x1 mm<sup>3</sup> were designed to fit the holders. The samples were cleaned immersed in acetone in an ultrasonic bath, then mounted into holders and pre-loaded (**Fig. 1**). A total of six specimens were loaded to the Yield Strength (YS). The load was applied by tightening holder screws at room temperature; the respective elastic deflection was calculated according to the ISO7539-2: 1989.

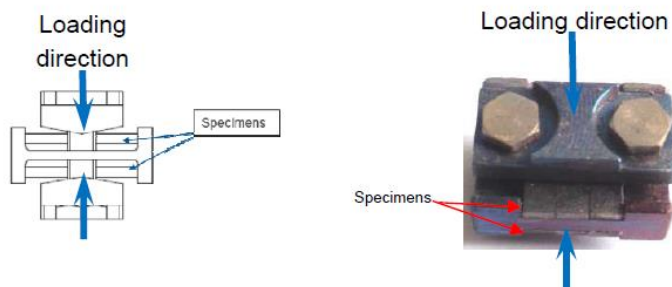


**Fig. 1** The scheme (left) and an actual photo (right) of specimen in the holder

Pre-loaded specimens were inserted in the LBE at 350°C for 2000 hours of exposure in a static tank. The concentration of dissolved oxygen in the liquid Pb-Bi was being changed by dosing of gases. The oxygen content was monitored by Bi/Bi<sub>2</sub>O<sub>3</sub> sensors; the measured concentration was oscillating within the range of 10<sup>-7</sup>-10<sup>-5</sup> wt. %. This level is sufficient to develop oxides on the steel [1, 7 and 18].

After the exposure, the specimens were observed and analysed using dual beam FIB-SEM system LYRA3 GMU (TESCAN). The sample cross-section, which is intercepting the steel-LBE interface in a reference position on the sample, was prepared and examined using secondary electron mode at accelerating voltage of 20 kV and electron beam current ~ 1 nA. The FIB milling and polishing procedure using Ga<sup>+</sup> ions was applied to produce the TEM lamella. Subsequent extraction of the lamella was done with a standard FIB lift-out technique. TEM observations of the lamella were carried out using the JEOL JEM 2200FS Field Emission Transmission Electron Microscope operated at 200 kV accelerating voltage. The structural and chemical composition of different features was analysed by the electron diffraction, EDS and then confirmed by EELS technique.

### 3 Results

After 2000h of exposure to LBE at 350°C, the T91 developed an oxide up to 1.5 μm with a two-layer structure (**Fig. 2**), which prevented the direct contact with the liquid metal. The oxide prevented both, material dissolution and crack initiation. For detailed characterization of the oxide layer formed at the interface, the TEM lamella was extracted from the cross-section region, which was then further studied by HR-STEM.

A protective Pt layer was deposited on the reference position of the sample. Rough milling of 10 μm long trenches at both sides of the lamella was performed using of 30 kV ion beam energy and ~ 1 nA ion current. When thinning and undercutting was done, the lamella was lifted-out by a nanomanipulator. Once attached to the TEM holder, the lamella was further thinned and finely polished using lower ion currents ~ 0.2 nA. To suppress the FIB-induced damage and Ga-

contamination of the sample, the final polishing was performed at low ion beam energy, 5 kV, and the final thickness was less than 100 nm.

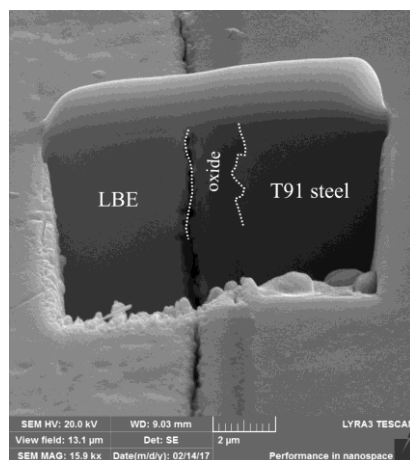


**Fig. 2** FIB-SEM cross-section image of the T91-liquid metal interface with a  $\sim 2 \mu\text{m}$  thick complex oxide layer in between

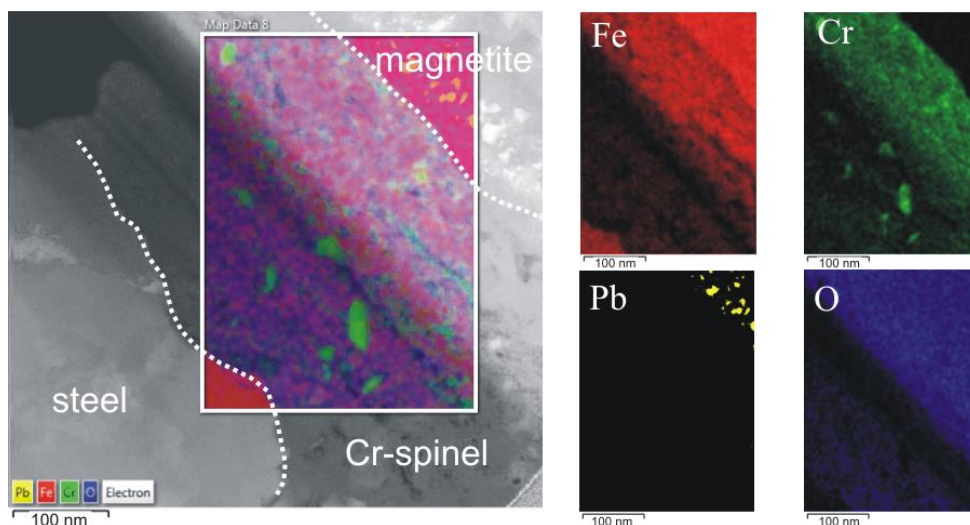


**Fig. 3** EDS X-ray elemental maps depicting the distribution of major elements within the oxides

During the HR-STEM analysis those two oxide layers grown on T91 matrix were confirmed and characterized more closely. From the different Z-contrast obtained by STEM HAADF detector is obvious, that these two oxide layers have a different chemical composition. The EDS maps (see **Fig. 3**) showed that the inner oxidation layer contained Fe-Cr-O elements, whereas the outer oxidation layer contained only Fe-O. The structure of both oxide layers was confirmed by selected area diffraction (SAED) as spinel  $\text{FeCr}_2\text{O}_4$  and magnetite  $\text{Fe}_3\text{O}_4$ , respectively (**Fig. 4**). To confirm the different chemical composition of both oxide layers, EELS measurements were also performed (**Fig. 4**).

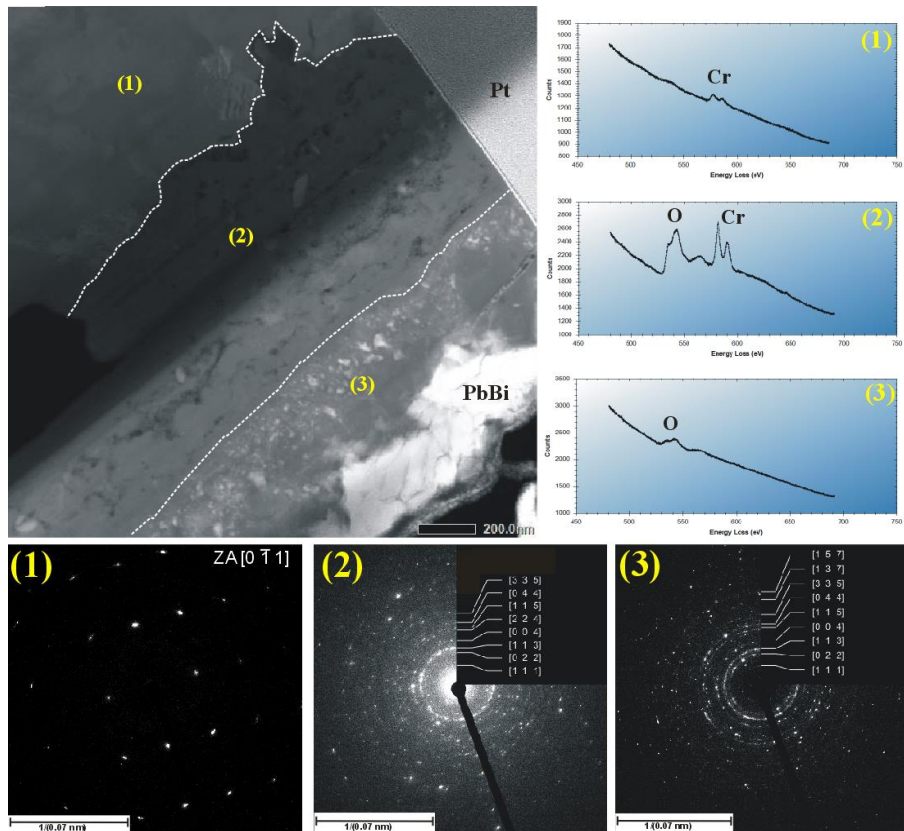


**Fig. 4** HAADF image of the TEM lamella shows the T91 steel (1) with a complex spinel (2) and magnetite oxide layer (3) preventing the direct contact with the liquid metal. SAED patterns of the matrix and oxides are at the bottom and corresponding EELS spectra giving more detailed structural-chemical information are on the left side

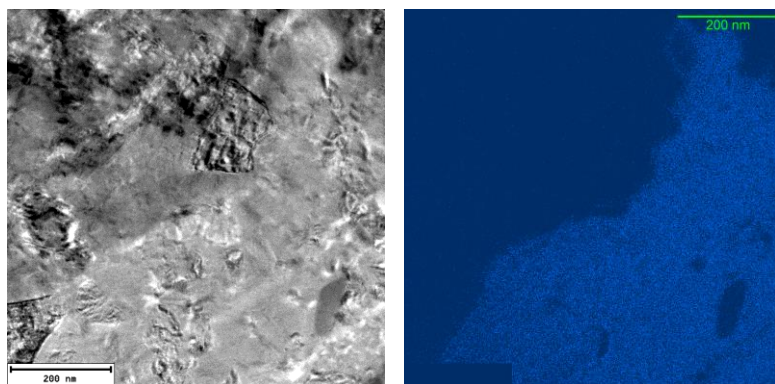


**Fig. 5** TEM image of the uneven matrix-oxide interface (left) and the EFTEM image of the same area showing the presence of oxygen in the structure (right)

The EFTEM imaging was used for a detailed and clear visualization of the boundary between matrix steel and the inner spinel layer. The EFTEM image contains only the O K-edge (532 eV)

signal is shown in **Fig. 5** (right). Definition of this boundary gives information about the role of the microstructure in the inner diffusion of oxygen. Detailed observation revealed also particles of  $\text{Cr}_{23}\text{C}_6$  present within the inner spinel layer (**Fig. 6**). Moreover, both Pb particles and Pb-Bi particles were identified in the outer magnetite layer.

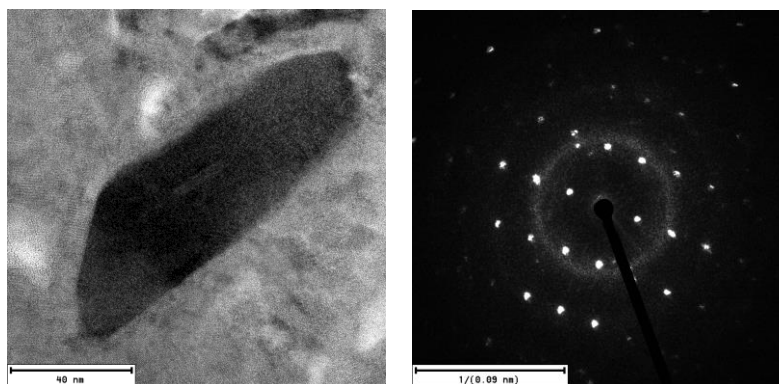


**Fig. 6** BF TEM image showing the particle of  $\text{Cr}_{23}\text{C}_6$  (left) and corresponding nano-beam diffraction (NBD) pattern (right)

#### 4 Discussion

This work shows experimental data obtained by the SEM-FIB that in conjunction with other advanced microscopic techniques allowed the observation of fundamental elements characterising oxides grown on the ferritic-martensitic steel in contact with LBE. The combination of conventional TEM techniques (BF imaging, SAED) with analytical capabilities of STEM-EDS and STEM-EELS allowed us to better understand the structural-chemical nature of the complex oxide layer. The utilisation of the nano-beam diffraction (or HR-TEM) enabled to characterize very small particles within the oxide scales [20].

The oxides developed under experimental conditions were sufficient to protect the steel T91 from the direct contact with the static liquid LBE. The oxidation process of the steel in contact with oxygen which contains LBE was extensively studied in [15-19]. The authors described the growth mechanism of a double-layer oxide. The oxide layer, which has a duplex structure, is composed of an internal Fe–Cr spinel layer and the external magnetite layer. The magnetite layer grows by iron diffusion in the outer direction at the LBE/oxide interface, whereas the Fe–Cr spinel layer grows, at the metal/magnetite interface, inside the space kept “available” by the iron vacancies accumulation due to iron outwards diffusion for magnetite formation. The limiting mechanism is the iron diffusion that allows the creation of available space for the Fe–Cr spinel growth [16]. According to these assumptions, the Fe–Cr spinel layer thickness depends on the capability of magnetite formation, which is also dependent on the oxygen content of the environment and on the microstructure of the surface layer. In our study, the composition and structure of the double-layer oxide corresponds with previously described models and observations [7, 8 and 18].

A faster oxygen diffusion and inward oxidation may take place along the grain boundaries and defects. Due to this fact, the grain size of the substrate could play a significant role in the diffusion controlled oxidation behaviour of steels. The uneven metal/oxide interface observed on the specimen indicates an intergranular oxidation mechanism, by which the oxide grows inward.

Further investigation of the steel/oxide interface is necessary for the evaluation of the role of grain boundaries during the oxidation process.

The observed embedded particles of Pb-Bi in the outer magnetite, and the presence of Cr-carbides in the inner spinel, have the potential to create internal stresses in the growing oxide layer. These impurities might cause time dependant damage of the oxide.

No cracks were found in studied specimens. The absence of cracking in these conditions is possibly due to lack of wetting [12-14] and the fact that the level of applied load was not sufficient to damage neither the surface of the steel nor the oxide formed during exposure. Oxides prevent corrosion/dissolution of steels in the liquid metal and serve as a barrier that prevents wetting, which is being considered as one of the assumptions for the LME initiation.

## 5 Conclusions

Specimens from the T91 pre-stressed to the yield strength was exposed to static Pb-Bi eutectic at 350°C for 2000h.

- A two-layer continuous oxide grew on the specimen surface. The outer layer was identified by TEM as magnetite and the inner one as Fe-Cr spinel.
- The applied experimental conditions were not sufficient to produce cracks in the oxide layer, no cracking was observed in the sample cross-section.
- FIB coupled with other advanced microscopic techniques (SEM, TEM, STEM-EELS, STEM-EDS, NBD, etc.) represent an effective tool for characterization of thin oxides from the morphological, elemental and structural point of view.
- The detailed TEM observation revealed impurities present within the oxide layers – particles of Cr<sub>23</sub>C<sub>6</sub> in spinel and Pb (Pb-Bi) clusters in magnetite.

## References

- [1] OECD/NEA: Handbook on Lead-bismuth Eutectic Alloy and Lead Properties, Materials Compatibility, Thermal hydraulics and Technologies, 2015, <https://www.oecd-nea.org/science/pubs/2015/7268-lead-bismuth-2015.pdf>. [Accessed 1 November 2017]
- [2] G. Grasso et al.: Nuclear Engineering and Design, Vol. 278, 2014, p.287-301, DOI:10.1016/j.nucengdes.2014.07.032
- [3] L. Cinotti, C.F. Smith, H. Sekimoto, L. Mansani, M. Reale, J.J. Sienicki: Journal of Nuclear Materials, Vol. 415, 2011, p.245-253, DOI:10.1016/j.jnucmat.2011.04.042
- [4] R. Ponciroli, A. Cammi, A. Della Bona, S. Lorenzi, L. Luzzi: Progress in Nuclear Energy, Vol. 85, 2015, p. 428-440, DOI:10.1016/j.pnucene.2015.06.024
- [5] R. Ganesan, T. Gnanasekaran, R.S. Srinivasa: Journal of Nuclear Materials, Vol. 349, 2006, p. 133-149, DOI:10.1016/j.jnucmat.2005.10.006
- [6] R.G. Ballinger, J. Lim: Nuclear Technology, Vol. 147, 2004, p. 418-435, DOI:10.13182/NT04-A3540
- [7] H. Glasbrenner, J. Konys, G. Mueller, A. Rusanov: Journal of Nuclear Materials, Vol. 296, 2001, p. 237-242, DOI:10.1016/S0022-3115(01)00522-0
- [8] G. Mueller et al.: Journal of Nuclear Materials, Vol. 335, 2004, p. 163-168, DOI:10.1016/j.jnucmat.2004.07.010
- [9] A. Heinzl, G. Müller, A. Weisenburger: Journal of Nuclear Material, Vol. 437, 2013, p. 116-121, DOI:10.1016/j.jnucmat.2013.01.298
- [10] F. Di Gabriele, A. Doubkova, A. Hojna: Journal of Nuclear Materials, Vol 376, 2008, p. 307-311, DOI:10.1016/j.jnucmat.2008.02.029

- [11] J.-B. Vogt, A. Verleene, I. Serre, A. Legris, *Journal of Nuclear Materials*, Vol. 335, 2004, p. 222-226, DOI:10.1016/j.jnucmat.2004.07.024
- [12] F. Di Gabriele, A. Hojna, M. Chocholousek, J. Klecka: *Metals*, Vol. 342, n. 7, 2017, p. 1-14, DOI:10.3390/met7090342
- [13] T. Auger et al.: *Journal of Nuclear Materials*, Vol. 415, 2011, p. 293-301, DOI:10.1016/j.jnucmat.2011.04.021
- [14] J. Van den Bosch, G. Coen, P. Hosemann, S.A. Maloy: *Journal of Nuclear Materials*, Vol. 429, 2012, p. 105-112 DOI:10.1016/j.jnucmat.2012.05.017
- [15] L. Martinelli, F. Balbaud-Célérier, A. Terlain, S. Delpech, G. Santarini, J. Favergeon, G. Moulin, M. Tabarant, G. Picard, *Corrosion Science*, Vol. 50, 2008, p. 2523–2536, DOI:10.1016/j.corsci.2008.06.050
- [16] L. Martinelli, F. Balbaud-Célérier, A. Terlain, S. Bosonnet, G. Picard, G. Santarini: *Corrosion Science*, Vol. 50, 2008, p. 2537–2548, DOI:10.1016/j.corsci.2008.06.051
- [17] L. Martinelli, F. Balbaud-Célérier, G. Picard, G. Santarini: *Corrosion Science*, Vol. 50, 2008, p. 2549–2559, DOI:10.1016/j.corsci.2008.06.049
- [18] A. Weisenburger et al.: *Journal of Nuclear Materials*, Vol. 415, 2011, p. 260- 269, DOI:10.1016/j.jnucmat.2011.04.028
- [19] A. Hojná, H. Hadraba, F. Di Gabriele, R. Husák, I. Kuběna, L. Rozumová, D. Marušáková: *Corrosion-mechanical behaviour of T91 and 9-20Cr ODS steels exposed to flowing lead-bismuth*, In.: *Materials structure & micromechanics of fracture*, Brno, June 27-29, 2016, p. 627-631
- [20] D. B. Williams, C. B. Carter: *Transmission Electron Microscopy A Textbook for Materials Science*. 2nd ed., New York: Springer Science+Business Media, New York, 2009

### Acknowledgements

*Parts of these activities were financially supported by the project GAČR-KAMILE c.n. 16-15008S. The presented work was financially supported by the Project CZ.02.1.01/0.0/0.0/15\_008/0000293: Sustainable energy (SUSEN) – 2nd phase, realized in the framework of the European Structural and Investment Funds.*